Footprint Catalysis. IV.[1,2,3] Structural Effects of Templates on Catalytic Behavior of Imprinted Footprint Cavities

Toyoshi Shimada, Kiyoko Nakanishi, and Kensaku Morihara*
Department of Chemistry, Faculty of Science, Nara Women's
University, Kitauoyanishi-machi, Nara 630

(Received October 28, 1991)

Footprint catalysts are silica(alumina)gel catalysts with tailored specificities. Their catalytic sites are "molecular footprint-like" cavities formed by a molecular imprinting procedure with templates, which are referred to as transition-state or reactive-intermediate analogs of the catalyzed reactions. To clarify the relationship between the structural feature of template molecules and catalytic behavior, seven footprint catalysts were prepared by imprinting with templates of several types closely related to the substrates, benzoic anhydride and acetic anhydride; their catalytic activity and thermodynamic parameters for 2,4-dinitrophenolysis were then estimated. Among these catalysts, a catalyst imprinted with *N,N′*-dibenzoylbenzenephosphonediamide, a tetrahedral intermediate analog for benzoic anhydride substrate, showed a 10-fold higher catalytic activity than did the other imprinted catalysts.

A novel strategy for tailor-made silica(alumina)gel catalysts has been developed under the name of "footprint catalysis" by the present authors.[1—3] This is based on the molecular imprinting with transition-state analogs as templates, and thus it might be, in a sense, referred to as a chemical version of attractive "catalytic antibodies".[4,5] A good amount of information concerning the required catalyst design have been accumulated during the course of our studies. The catalytic sites of the footprint catalysts are characteristic cavities with fine complementarity to the templates used in imprinting. The cavities, thus formed, can stabilize the transition state of the substrate molecules by specific interaction through "complementarity" to exhibit enzyme-like catalysis. The term "complementarity" has a dual meaning, i.e., "electronic" and "geometric";[1] the former serves mainly as the Lewis acid character and provides an acid-catalytic ability of the cavities; the latter provides a fine molecular recognition capability due to their inclusion and exclusion effects.[2] The cooperation of Lewis acidity and the molecular recognition capability should create a characteristic catalysis. However, the fundamental question as to where a Lewis acid site (Al atom isomorphically incorporated into silicate matrix) is located in a footprint cavity has not yet been clearly answered: This is because the template molecules of the Lewis base character, so far as used in imprinting, are ambiguous lone pair donors and, consequently, the geometry of the induced footprint cavities of the Lewis acid character also remains ambiguous. In order to characterize the true feature of the footprint cavities, i.e., the location of a Lewis acid site in a cavity and the geometry around the acid site, substrate specificity and inhibition studies were carried out and thermodynamic considerations were made.

Experimental

Materials. All of the chemicals were of guaranteed grade from Nacalai Tesque Co., Ltd., if not otherwise specified.

Templates and Inhibitors: *N*-Acetylbenzamide ($PhCONHCOCH_3$),[2] **1**, mp 116—117 °C (lit,[6] 115 °C); (Found: C, 66.25; H, 5.52; N, 8.58%).

N-Acetylbenzenesulfonamide ($PhSO_2NHCOCH_3$),[2] **2**, mp 125—126 °C; ^1H NMR ($CDCl_3$) δ=9.47 (s, 1H,-NH-), 7.96 (m, 2H, ArH), 7.61 (m, 3H, ArH), 2.05 (m, 3H, CH_3CO-); (Found: C, 48.38; H, 4.57; N, 7.00%).

N-Methylsulfonylbenzamide ($PhCONHSO_2CH_3$), **3**; prepared by metalation of methylsulfonylamide with sodium hydride followed by acylation with benzoyl chloride, and recrystallized from water, mp 153—156 °C. Yield was 15%. IR (KBr) 3235 (N-H), 1680 (C=O), 1247 (amide III), 1175 (SO_2); ^1H NMR ($CDCl_3$) δ=8.59 (s, 1H, NH), 7.87—7.49 (m, 5H, ArH), 3.45 (s, 3H, CH_3-); (Found: C, 47.71; H, 4.55; N, 7.35%).

N-Benzoylbenzenesulfonamide ($PhCONHSO_2Ph$),[1] **4**, mp 148 °C (lit,[7] 147 °C); (Found: C, 59.51; H, 4.26; N, 5.37%).

N,N′-Dibenzoylbenzenephosphonediamide ($PhPO(NHCOPh)_2$), **5**; To benzenephosphonediamide (7.80 g, 50.0 mmol) dissolved in 200 cm^3 of THF, was added sodium hydride (oil suspension of 60% purity, 5.0 g, 125 mmol) under stirring at 50 °C. After 10 min, benzoic anhydride purified by recrystallization from benzene-petr. benzine (22.6 g, 100 mmol) was added and allowed to react at room temperature for 12 h. The reaction mixture was evaporated to dryness, and the residue was dissolved in water (300 cm^3). The solution was brought to pH 5 in order to precipitate the product, which was collected by filtration and recrystallized from ethanol with 35% yield. mp 211 °C; IR (KBr) 3232 (N-H), 1685 (C=O), 1195 (P=O); ^1H NMR ($CDCl_3$-DMSO-d_6=9 : 1) δ=10.5 (d, 2H, -NH-), 8.02 (m, 6H, ArH), 7.56 (m, 9H, ArH); (Found: C, 65.83; H, 4.79; N, 7.79%)

N-Benzoyl-2,4-dinitroaniline ($PhCONH(2,4\text{-}NO_2)Ph$), **6**; prepared by acylation of 2,4-dinitroaniline with benzoyl chloride and catalytic amount of concd sulfuric acid, and recrystallized from acetic acid. mp 206—208 °C (lit,[8] 201—202 °C). ^1H NMR ($CDCl_3$) δ=11.66 (s, 1H, NH), 9.35—7.57 (m, 8H, ArH).

Dibenzamide ($PhCONHCOPh$),[1] **7**; mp 145.5—148 °C (lit,[9] 148 °C); (Found: C, 74.81; H, 4.88; N, 6.14%)

Benzamide, **8**, and Benzenesulfonamide, **9**, were of guaranteed grade of Nacalai Tesque Co., Ltd. and used without further purification.

Benzenephosphonediamide ($PhPO(NH_2)_2$), **10**; prepared by ammonolysis of phenylphosphonic dichloride with aqueous ammonia, and recrystallized from ethanol mp 191 °C (lit, [10] 189 °C).

Silica Gel; Merck Kieselgel 60, art.no. 7754, particle size 0.06—0.20 mm, mesh 70—230, was used.

Substrate; Benzoic anhydride was recrystallized from benzene-petr. benzine, mp 42 °C. Acetic anhydride over anhydrous sodium acetate (20 g per 1 dm^3 of acetic anhydride) was distilled under reduced pressure.

Nucleophile: Potassium 2,4-dinitrophenolate, prepared as previously reported,[3] was recrystallized from water.

Catalysts: The preparation procedures and acid site characterization of the catalysts were the same with those previously described,[1] except for the use of different compounds as templates. The control catalyst stemmed from the aluminium ion-doped gel and lacked only imprinting with a template, and possessed native Lewis acid sites without any cavity structure.

Kinetic Measurement: The reaction conditions and procedures were the same as those previously reported,[3] i.e., 2,4-dinitrophenolysis of benzoic anhydride and acetic anhydride at 30 °C in anhydrous acetonitrile. Pseudo-first-order rate constants, k_{obs}, were calculated from the decrease in the O.D. at 430 nm, and K_m, $V_{max}(=k_{obs}$ maximum) and K_i were obtained as usual from a double reciprocal plot in the Michaelis–Menten equation.

Results and Discussion

Substrate Specificities: Three footprint catalytic cavities were imprinted with templates **1**, **2**, and **3**; their substrate specificities(k_{cat}/K_m) were then estimated. This study was based on the finding that some footprints differentiate a methyl group from a phenyl group, and vice versa,[2] and that these molecular recognition capabilities are revealed in substrate specificities.[3] In order to determine the location of the Lewis acid sites and to compare the ability of the carbonyl and sulfonyl groups for Lewis acid site formation, the templates were designed by combining the benzoyl or benzenesulfonyl moieties with the acetamido or methylsulfonamido moieties, respectively. As can be seen in Table 1, no significant difference was found in the substrate specificity(k_{cat}/K_m) toward benzoic anhydride and acetic anhydride for a catalyzed reaction by the control catalyst, whereas, significant differeces were observed among the catalyzed reactions by the catalysts imprinted with **1**, **2**, and **3**, (hereafter referred as {**1**}, {**2**}, and {**3**}), respectively. Differences in the relative ratio in the specificities (benzoic/acetic) of {**1**}, {**2**}, and {**3**} clearly demonstrate that {**1**} prefers benzoic anhydride, and that {**2**} and {**3**} prefer acetic anhydride to the other. These specificities are manifest in the K_m values, rather than k_{cat}s, and apparently originate from the molecular recognition capability of the footprint cavities. This finding suggests that, to fit better to substrate molecules, the Lewis acid site in {**1**} is located close to the partial structure(subsite) for a phenyl group, and those of {**2**} and {**3**} are located close to the subsite for a acetyl group. The possibility that amide N might act as the lone pair donor has been excluded; {**7**}, cavities imprinted with dibenzamide, were found to be competitively inhibited with the amide-lacking dibenzoylmethane,[2] and, furthermore, cavities imprinted with the amide-lacking bis-(benzenesulfonyl)methane showed catalysis for benzoic anhydride.[11] Therefore, the true lone pair donor in **1** is surely carbonyl O of the benzoyl group, that in **2** is carbonyl O of the acetyl group, and that in **3** is sulfonyl O of methylsulfonyl group. These

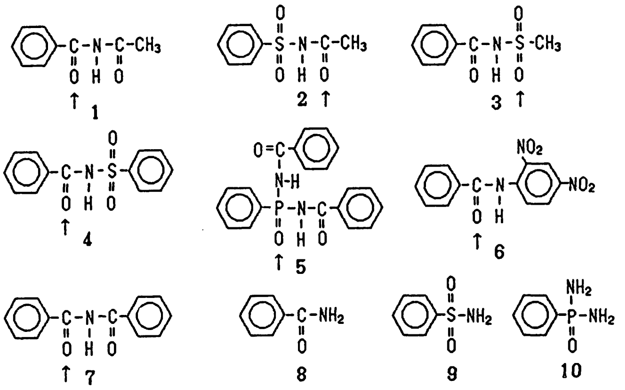

Fig. 1. Template molecules and inhibitors.
The arrows indicate the location of a Lewis base site in the template molecules.

Table 1. Kinetic Parameters of the Catalyzed Reactions by Footprints {**1**}, {**2**}, {**3**}

Catalyst imprinted with { }	Substrate	$10^{-2}\times k_{cat}$ [a)] $M^{-1}s^{-1}$	$10^4\times K_m$ M	$10^{-5}\times k_{cat}/K_m$ $M^{-2}s^{-1}$	$10^4\times k_{obs.max}$ [b)] s^{-1}	$k_{obs.max}/K_m$ $M^{-1}s^{-1}$	(K_m) [c)]	(k_{cat}/K_m) [c)]
{**1**, $PhCONHCOCH_3$}	Bz_2O	1.89	2.70	7.00	6.62	2.45	(0.34)	(2.98)
	Ac_2O	2.38	6.31	3.77	8.33	1.32	(0.80)	(1.47)
{**2**, $PhSO_2NHCOCH_3$}	Bz_2O	2.66	8.51	3.13	9.30	1.09	(1.08)	(1.33)
	Ac_2O	2.77	5.72	4.84	9.67	1.69	(0.73)	(1.88)
{**3**, $PhCONHSO_2CH_3$}	Bz_2O	2.45	5.54	4.42	8.57	1.55	(0.70)	(1.88)
	Ac_2O	2.40	4.03	5.96	8.38	2.08	(0.51)	(2.32)
Control	Bz_2O	1.86	7.91	2.35	6.51	0.82	(1.00)	(1.00)
	Ac_2O	2.01	7.83	2.57	7.03	0.90	(1.00)	(1.00)

a) Calculated with the molarities of catalytic sites per *g* determined by titration using pyridine poisoning.[3] b) The values of $k_{obs.max}$ indicate the intercepts of Lineweaver–Burk plots on coordinate axis. c) Figures in parentheses mean normalized values obtained by dividing with the corresponding values of the control catalyst.

Table 2. Kinetic Parameters of the Catalyzed Reactions by Footprints {**4**}, {**5**}, {**6**}, {**7**}

Catalyst imprinted with { }	$10^{-2}\times k_{cat}$	$10^4\times K_m$	$10^{-5}\times k_{cat}/K_m$	$10^6\times K_i$ by **4**	$10^6\times K_i$ by **5**	$10^6\times K_i$ by **8**	$10^6\times K_i$ by **9**	$10^6\times K_i$ by **10**
	$M^{-1}s^{-1}$	M	$M^{-2}s^{-1}$	M	M	M	M	M
Control	3.41	11.38	3.00	No inhibition by **4**,**5**,**6**,**7**,**8**,**9**,**10**.				
{**4**, $PhCONHSO_2Ph$}	3.27	3.78	8.64	2.22	n.d.	2.91	6.68	6.40
{**5**, $PhPO(NHCOPh)_2$}	33.36	4.06	82.23	1.99	20.5	8.30	n.d.	3.80
{**6**, $PhCONH(2,4\text{-}NO_2)Ph$}	4.31	4.07	10.06					
{**7**, PhCONHCOPh}	2.81	2.64	10.66					

n.d.: not determined.

findings also suggest that the Lewis acid forming abilities of the two groups, sulfonyl and carbonyl, do not depend on only the characteristics of functional group itself, but on their position in the template molecules.

Competitive Inhibition Study. To clarify the location of a Lewis acid site as well as its neighboring space in {**4**} and {**5**}, the preceding substrate specificities study could not be applied because **4** and **5** lack acetyl groups, and then inhibition studies with inhibitors of a moiety of template molecules, **8**, **9**, **10**, and with the original templates, **4** and **5**, were carried out, as shown in Table 2. Template **4** has been referred to as an analog of a tetrahedral intermediates[1)] closely resembling to the transition state of the catalyzed reaction, and was used often during the course of our studies;[1-3)] the preceding specificity study, however, revealed that the sulfonyl group cannot always induce a Lewis acid site in preference to a carbonyl group, and reinvestigation of {**4**} is thus required to determine the geometry of the cavity. Although template **4** should be an analog for a reactant-like transition state if carbonyl O is the true lone pair donor, it should be an analog for the tetrahedral intermediate if sulfonyl O is the donor. Newly introduced template **5** is an analog of the phosphonyl substitute of **4**, and is a tetrahedral intermediate analog if the phosphonyl group is the true lone pair donor. Template **6** is a product-like and **7** is a reactant-like transition state analog; inhibitor **8** is a moiety of **4**, **5**, **6**, and **7**, inhibitor **9** is that of **4**, and inhibitor **10** is that of **5**, respectively. As can be seen in Figs. 2 and 3, all of the catalyzed reactions show typical competitive inhibition plots. The observed coincidence of the intercepts of all of the Lineweaver–Burk plots on the coordinate axis demonstrates that all of the inhibitors are bound onto the same catalytic sites, in spite of their different structures. This fact enables a quantitative comparison of the affini-

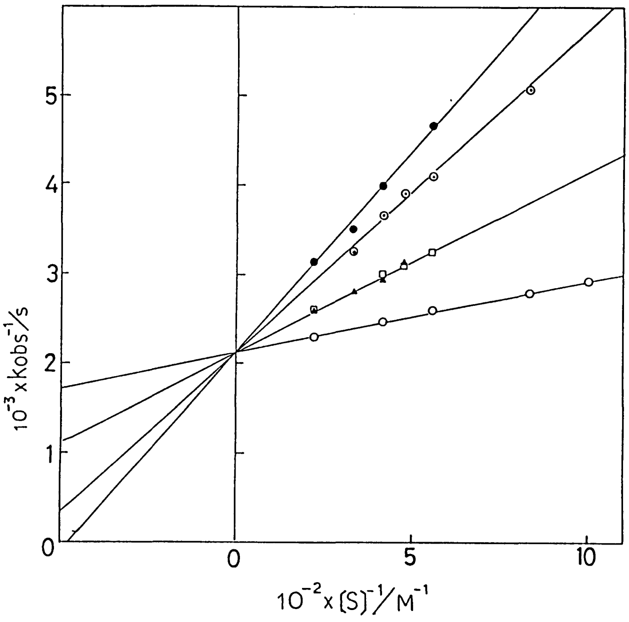

Fig. 2. Competitive inhibition of a footprint catalyst {**4**} by **4**, **8**, **9**, **10**.
[S]: benzoic anhydride concentration. [I]: inhibitor concentration.
○: [I]=0. ●: [I]=1.0×10^{-5} M (**4**). ⊙: [I]=1.0×10^{-5} M (**8**). ▲: [I]=1.0×10^{-5} M (**9**). □: [I]=1.0×10^{-5} M (**10**).

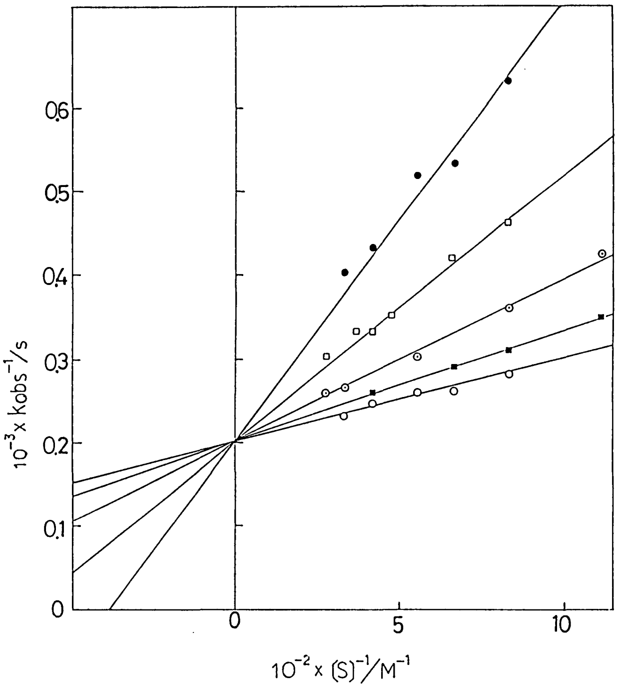

Fig. 3. Competitive inhibition of a footprint catalyst {**5**} by **4**, **5**, **8**, **10**.
[S]: benzoic anhydride concentration. [I]: inhibitor concentration.
○: [I]=0. ●: [I]=1.0×10^{-5} M (**4**). ■: [I]=1.0×10^{-5} M (**5**). ⊙: [I]=1.0×10^{-5} M (**8**). □: [I]=1.0×10^{-5} M (**10**).

ties of these inhibitors to the footprint cavities, i.e., the molecular recognition capability $(-\Delta G^0 RT \ln (1/K_i))$ of a footprint cavity. As shown in Table 2, the magnitude of the affinities of the inhibitors to {**4**} are in the order **4**>**8**>**9**=**10**. The highest affinity of **4** to {**4**} comes from the maximum interaction between a footprint cavity and its original template, whereas the smaller magnitudes of the affinities of **8**, **9**, and **10** to {**4**} are caused by "partial affinities" which result from a partial interaction between part of a footprint and the moiety of the inhibitor (partial footprint effect.[2]) The magnitude of these "partial affinities" greatly depends on the fitting mode of an inhibitor with the space neighboring a Lewis acid site; the geometry of the cavity can thus be speculated from the magnitude of the observed affinities. The fact that **8** has a greater affinity than do **9** and **10** to {**4**}, indicates that the space neighboring the Lewis acid site of {**4**} is better fitted to **8** than to **9**; this means that the acid site of {**4**} is never inductively formed by the benzenesulfonyl moiety of the template **4**, as was once assumed,[1] but instead is formed by its benzoyl moiety in the imprinting process. Furthermore, since the carbonyl carbon of the benzoyl moiety has the sp^2 configuration, the {**4**} formed by the benzoyl moiety should involve a plane space near the acid site and would presumably favor a reactant-like transition state of the sp^2 configuration, rather than intermediate possessing sp^3 configuration. This speculation is otherwise supported by the following. The inhibitor **10** with phosphonyl P of the sp^3 configuration, like **9**, also shows less affinity to {**4**} than does **8**; also, no remarkable difference in the catalytic behavior has been observed between {**4**} and {**7**} in studies carried out so far; the latter should apparently have a catalytic cavity for the reactant-like transition state of sp^2. The inhibitors, **9** and **10**, cannot lie in the cavity apart from the Lewis acid site to afford a competitive inhibition, since the magnitude of such binding without acid-base complexation should give a far smaller affinity than that on the acid site.[2] Concerning the inhibition of {**5**}, the magnitudes of the affinities are in the order **4**>**10**>**8**>**5**. The order **10**>**8** is in reverse to that observed regarding inhibition of {**4**}. A CPK model examination exhibits that **5** can assume two adsorption modes during imprinting and inhibition: one involves contact with a cavity through the Bz-NH-PO-NH-Bz moiety; the other is that through the Ph-PO-NH-Bz moiety. The latter one is more likely because **4** and the substrate, benzoic anhydride, which resemble Ph-PO-NH-Bz in shape, were found to adsorb tightly on {**5**}. Hence, a similar consideration to that concerning {**4**}, as mentioned above, is reasonable, leading to the conclusion that the Lewis acid site of {**5**} is inductively imprinted with the phosphonyl O of Ph-PO-NH-Bz and, thereby, the space neighboring the acid site is not a plane, but is complementary to a tetrahedral phosphonyl group; {**5**} prefer a tetrahedral intermediate to a plane reactant-like transition state in order to reveal its efficient catalysis. It should be noted that the highest $k_{\mathrm{cat}}/K_{\mathrm{m}}$ value of {**5**} is not brought about by a binding step (K_{m}), but is caused by a catalytic step (k_{cat}). Although such rate enhancement is widely observed in the specific catalysis of enzymes,[12,13] it was observed for the first time in footprint catalysis. The unusual lower affinity of {**5**} observed to the original template **5** is probably due to the solvation of another moiety of **5**, -NH-Bz, apart from the cavity; when put into bulk acetonitrile it might weaken the binding of **5** to {**5**}.

Thermodynamic Aspect of the Catalyses by Cavities and General Discussion. The activation parameters of three footprint cavities and the control catalytic sites for the catalytic step, E_{a}, $\Delta H^{\ddagger}$, $\Delta S^{\ddagger}$, $\Delta G^{\ddagger}$, and that for the overall reaction, $\Delta G^{\ddagger}_{\mathrm{total}}$, and standard free energy change in the binding step, $\Delta G^0_{\mathrm{ass}}$, were determined over the temperature range 9 to 35 °C; the results are summarized in Table 3. Assuming that K_{m} is nearly the same as the dissociation constant, K_{s}, and that the solvation effect of acetonitrile is small,[3,14] the binding energy of the substrate molecules to catalytic sites can be evaluated from the values of $-\Delta G^0_{\mathrm{ass}}(=RT \ln K_{\mathrm{m}}^{-1})$. The results, shown in Table 3, demonstrate that the three footprint catalytic cavities, {**4**}, {**5**} and {**6**}, have a distinctly smaller $\Delta G^0_{\mathrm{ass}}$ than does that of the control catalyst, the substrate molecules being bound specifically and more tightly (2.77 kJ mol^{-1}) to the footprint cavities through the "footprint effect", the complementary interaction. The differences seen among the three footprint catalytic cavities, however, are very small (0.18 kJ mol^{-1}), compared to the differences seen between the control and the footprint cavities (2.59 to 2.77 kJ mol^{-1}). On the other hand, various differences (−2.66 to −8.34 kJ mol^{-1}) are observed among the activation free energy

Table 3. Activation Parameters for 2,4-dinitrophenolysis of Benzoic Anhydride

Catalyst imprinted with { }	E_{a}	$\Delta H^{\ddagger\,\mathrm{a)}}$	$-\Delta S^{\ddagger\,\mathrm{a,b)}}$	$\Delta G^{\ddagger\,\mathrm{a)}}$	$\Delta G^{\ddagger}_{\mathrm{total}}$ c)	$-\Delta G^0_{\mathrm{ass}}$ d)
	kJ K^{-1} mol^{-1}	kJ mol^{-1}	J K^{-1} mol^{-1}	kJ mol^{-1}	kJ mol^{-1}	kJ mol^{-1}
Control	19.31	16.79	141	59.56	42.48	17.08
{**4**, $PhCONHSO_2Ph$}	16.56	14.04	151	59.67	39.82	19.85
{**5**, $PhPO(NHCOPh)_2$}	12.41	9.89	145	53.81	34.14	19.67
{**6**, $PhCONH(2,4\text{-}NO_2)Ph$}	7.67	5.15	178	58.97	39.30	19.67

a) Activation parameters for the catalytic step. b) Calculated by the values of $\Delta H^{\ddagger}$ and $\Delta G^{\ddagger}$. c) Activated free energy for the overall reaction. d) Standard free energy change in the binding step.

changes for the overall footprint-catalyzed reactions, $\Delta G^{\ne}_{\text{total}}(=-RT \ln k_{\text{cat}}/K_{\text{m}})$, i.e., -2.66 kJ mol^{-1} for (**4**) ($=39.82-42.48$ kJ mol^{-1}), -8.34 kJ mol^{-1} for {**5**}, and -3.18 kJ mol^{-1} for {**6**}. The small difference in $\Delta G^{\ne}_{\text{total}}$, -2.66 kJ mol^{-1} between {**4**} and the control is comparable to that in $-\Delta G^{0}_{\text{ass}}$, -2.77 kJ mol^{-1} ($=17.08-19.85$ kJ mol^{-1}), between them, which suggests that {**4**} is an apparent catalyst that exhibits catalysis mainly by a binding of the substrate onto it. In contrast to {**4**}, the large difference between {**5**} and the control, -8.34 kJ mol^{-1} ($=34.14-42.48$ kJ mol^{-1}), compared to the $-\Delta G^{0}_{\text{ass}}$, -2.59 kJ mol^{-1}, demonstrates that {**5**} displays intrinsic catalysis characteristics; {**5**} must have a mechanism to use a part of the binding energy for reducing the energy barrier along the reaction pathway. Thus, {**6**} with a difference, -3.18 kJ mol^{-1} in $\Delta G^{\ne}_{\text{total}}$ is likely to be similar to {**4**}.

The above-mentioned speculation is supported by an examination of the activation parameters, $\Delta H^{\ne}$, $\Delta S^{\ne}$, and $\Delta G^{\ne}$. Firstly, as shown in Table 3, the $\Delta G^{\ne}$s of the control-catalyzed and the {**4**}-catalyzed reactions are identical within experimental error; their contents, $\Delta H^{\ne}$s and $\Delta S^{\ne}$s, however, are evidently different. The more favorable $\Delta H^{\ne}$ of {**4**} by -2.75 kJ mol^{-1} for the reaction, compared to that of the control, is nearly cancelled out by the unfavorable $\Delta S^{\ne}$, by 10 J K^{-1} mol^{-1}, to give a nearly identical $\Delta G^{\ne}$. This indicates that the substrate molecules might bind to {**4**} possessing a favorable fitting space for a reactant-like transition state of the reaction and, thereby, might be retarded in turn in the restrictive transformation process to yield the identical $\Delta G^{\ne}$. Secondly, the more favorable $\Delta H^{\ne}$, by -6.90 kJ mol^{-1}, of {**5**} is never cancelled by the also favorable $\Delta S^{\ne}$ by 4 J K^{-1} mol^{-1}, to give the smallest $\Delta G^{\ne}$; the distinct rate enhancement thus actually originates in the catalytic process. This observation is consistent with the speculation that {**5**} might adsorb substrate molecules using the fitting space for the sp^3 configuration to stabilize the tetrahedral intermediate so as to give rise to an effectively catalyzed reaction. Thirdly, the most favorable $\Delta H^{\ne}$, by -11.64 kJ mol^{-1}, of {**6**} is cancelled by the most unfavorable $\Delta S^{\ne}$, by 37 J K^{-1} mol^{-1}. This might be explained if it is assumed that a strong binding of the substrate-nucleophile complex due to polar dinitrophenolate moiety takes place to affording a favorable $\Delta H^{\ne}$, and then a subsequent restrictive reorientation occurs to fit to the cavities for a product-like transition state, giving the unfavorable $\Delta S^{\ne}$.

In conclusion, the above-mentioned investigation has revealed the features of specific catalyses due to footprint cavities based on their precise molecular recognition. Although these catalyses are characteristic in biocatalysts, such as enzymes and catalytic antibodies, they are unprecedented in abiotic catalysts. The observations in the present study can provide fundamental knowledge concerning how to design appropriate template molecules for highly effective tailor-made catalysts, such as the proper use of **5** as a template resulting in a 10-fold higher catalytic efficiency than ever obtained before.

The authors would like to thank Dr. Takashi Nakazawa for his helpful advice and NMR measurements.

References

1) Part I: K. Morihara, S. Kurihara, and J. Suzuki, *Bull. Chem. Soc. Jpn.*, **61**, 3991 (1988).

2) Part II: K. Morihara, E. Nishihata, M. Kojima, and S. Miyake, *Bull. Chem. Soc. Jpn.*, **61**, 3999 (1988).

3) Part III: K. Morihara, E. Tanaka, Y. Takeuchi, K. Miyazaki, N. Yamamoto, Y. Sagawa, E. Kawamoto, and T. Shimada, *Bull. Chem. Soc. Jpn.*, **62**, 499 (1989).

4) R. A. Lerner and A. Tramontano, *Sci. Am.*, **258**, 42 (1988).

5) P. G. Schlutz, *Acc. Chem. Res.*, **22**, 287 (1989).

6) "Beilstein Handbuch der Organischen Chemie," Vol. IX, p. 213.

7) "Beilstein Handbuch der Organischen Chemie," Vol. XI, p. 43.

8) "Beilstein Handbuch der Organischen Chemie," Vol. XII, p. 754.

9) "Beilstein Handbuch der Organischen Chemie," Vol. IX, p. 213.

10) "Beilstein Handbuch der Organischen Chemie," Vol. XVI, p. 805.

11) K. Morihara, Y. Shimada, and T. Shimada, unpublished data.

12) W. P. Jencks, *Adv. Enzymol.*, **43**, 219 (1975).

13) A. Fersht, "Enzyme Structure and Mechanism," Freeman and Co., Ltd., San Francisco (1977).

14) Viktor Gutmann, "The Donor-Acceptor Approach to Molecular Interactions," Plenum Press, New York (1978), Chap. 2.